

# Nanoscale

Accepted Manuscript



This is an *Accepted Manuscript*, which has been through the Royal Society of Chemistry peer review process and has been accepted for publication.

*Accepted Manuscripts* are published online shortly after acceptance, before technical editing, formatting and proof reading. Using this free service, authors can make their results available to the community, in citable form, before we publish the edited article. We will replace this *Accepted Manuscript* with the edited and formatted *Advance Article* as soon as it is available.

You can find more information about *Accepted Manuscripts* in the [Information for Authors](#).

Please note that technical editing may introduce minor changes to the text and/or graphics, which may alter content. The journal's standard [Terms & Conditions](#) and the [Ethical guidelines](#) still apply. In no event shall the Royal Society of Chemistry be held responsible for any errors or omissions in this *Accepted Manuscript* or any consequences arising from the use of any information it contains.



## Nanoscale

## COMMUNICATION

## The Fate of Nano-Silver in Aqueous Media

Blake. J. Plowman,<sup>a</sup> Kristina Tschulik,<sup>\*a</sup> Emily Walport,<sup>b</sup> Neil P. Young<sup>b</sup> and Richard G. Compton<sup>\*a</sup>Received 00th January 20xx,  
Accepted 00th January 20xx

DOI: 10.1039/x0xx00000x

www.rsc.org/

Silver nanoparticles offer highly attractive properties for many applications, however concern has been raised over the possible toxicity of this material in environmental systems. While it is thought that the release of Ag<sup>+</sup> can play a crucial role in this toxicity, the mechanism by which the oxidative dissolution of nano-silver occurs is not yet understood. Here we address this through the electrochemical analysis of gold-core silver-shell nanoparticles in various solutions. This novel method allows the direct quantification of silver dissolution by normalisation to the gold core signal. This is shown to be highly effective at discriminating between silver dissolution and the loss of nanoparticles from the electrode surface. We evidence through this rigorous approach that the reduction of O<sub>2</sub> drives the dissolution of nano-silver, while in the presence of Cl<sup>-</sup> this dissolution is greatly inhibited. This work is extended to the single nanoparticle level using nano-impact experiments.

## Introduction

Silver nanoparticles represent a very important class of materials, having demonstrated altered optical, catalytic and biocidal properties relative to bulk silver.<sup>1</sup> This latter property has been extensively utilised in the fabrication of materials which inhibit the growth of bacteria and fungi in clothing or food storage containers, or by aiding wound healing when incorporated into bandages.<sup>2</sup> While such biocidal properties are clearly beneficial in a wide variety of applications, these properties may also lead to undesired environmental impacts as the nanoparticles are transferred from these materials to the environment through means such as mechanical wear, cleaning or their end of life disposal.<sup>3</sup>

Much attention has been directed towards the possible toxicology of silver nanoparticles, which has been claimed for algae, bacteria, fungi and fish, as have possible health impacts

towards humans.<sup>1,4,5</sup> While research has pointed to the toxicity of the nanoparticles themselves through their interaction with cell walls or by aiding the generation of reactive oxygen species (ROS),<sup>6,7</sup> it has also been reported that the toxicity of the silver nanoparticles might be imparted through the release of Ag<sup>+</sup> formed through the oxidative dissolution of the nanoparticles.<sup>7,8</sup>

Understanding the physico-chemical properties of the nanoparticles is therefore of great importance in order to predict the conditions under which the nanoparticles will react and release Ag<sup>+</sup>. However research in this field has attracted debate over a number of key issues, including the nature of the redox reactions which drive the dissolution of silver, as this oxidative process must occur concomitantly with the reduction of a suitable agent. A number of species have been proposed for this process including oxygen and/or hydrogen peroxide,<sup>4</sup> however as the concentrations of the relevant species are often unreported and debate exists over the possible formation of silver oxide as a reaction intermediate<sup>5,8-10</sup> it is clear that the mechanism has not yet been well established. The influence of halide ions has caused additional controversy, as it has been reported to either enhance or impede silver dissolution.<sup>9-12</sup> Note that the direct comparison of results is often challenging,<sup>13</sup> given that the data is obtained from a wide variety of experimental conditions (including different nanoparticle sizes, capping agents, surface charges and electrolytes) and the concentration of O<sub>2</sub> is often not reported.<sup>11</sup> As a result rigorous studies of the stability of silver nanoparticles, factoring in the role of O<sub>2</sub> and halides, are required to better understand the fate of silver nanomaterials in a wide variety of conditions.<sup>14</sup>

In this work we address these issues by exploring the stability of nano-silver through the electrochemical analysis of core-shell nanoparticles. This novel and rigorous approach allows the chemical stability of the silver shells to be investigated electrochemically after exposing the nanoparticles to the desired species (Figure 1). A key aspect of this method is the presence of the gold cores, which allows the number of nanoparticles remaining on the surface to be

<sup>a</sup> Department of Chemistry, PTCL, University of Oxford, South Parks Road, Oxford, OX13QZ, United Kingdom. E-mail: tschulik.kristina@gmail.com, richard.compton@chem.ox.ac.uk

<sup>b</sup> Department of Materials, University of Oxford, Parks Road, Oxford, OX13PH, United Kingdom.

<sup>†</sup> Electronic Supplementary Information (ESI) available: Determination of oxygen concentrations and further experimental details. See DOI: 10.1039/x0xx00000x

assessed. Thus a decrease in the silver oxidation charge due to particle loss from the electrode surface can be delineated from silver dissolution. This straight-forward and highly effective approach may be readily applied for the direct quantification of silver dissolution or passivation under a wide variety of conditions, leading to a better understanding of the behaviour of silver nanoparticles in environmental systems. In addition the study of such processes at an individual nanoparticle level is demonstrated through nanoparticle impact experiments, showing that this approach can directly address the dissolution of individual nanoparticles.

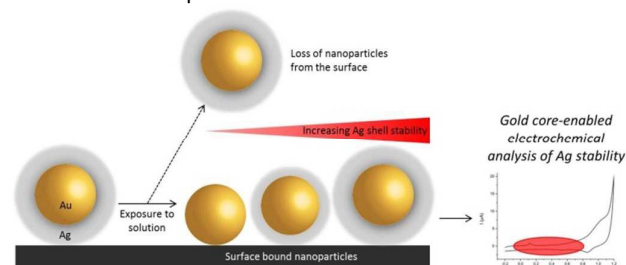


**Figure 1.** Schematic representation showing the electrochemical analysis of nano-silver using gold-core silver-shell nanoparticles.

## Experimental

Electrochemical measurements were performed using a  $\mu$ Autolab II (Metrohm) potentiostat with a temperature controlled Faraday cage ( $25 \pm 0.2$  °C). A three electrode system was used, with a platinum counter electrode and a saturated calomel reference electrode (SCE, saturated KCl) for voltammetry in solutions of NaCl or HCl, or a mercury/mercurous sulphate reference electrode (MSE, saturated  $K_2SO_4$ , measured at +0.399 V vs SCE) for voltammetry in  $NaNO_3$  and  $HNO_3$  solutions. All potentials referenced in this work are quoted versus SCE unless otherwise stated. Working electrodes consisted of glassy carbon plates (HTW) masked with Kapton tape leaving defined circular regions exposed (4 mm diameter), upon which  $2 \mu L$  of cetyl trimethylammonium bromide (CTAB) capped gold-core (35 nm diameter) silver-shell (thickness of 7.5 nm) nanoparticles (Nanopartz) were drop cast for voltammetry in 20 mM NaCl, 0.1 M  $NaNO_3$  and 0.1 M HCl, or  $8 \mu L$  in the case of 0.1 M  $HNO_3$ . For nano-impact experiments carbon fibre microcylinder electrodes were used, fabricated according to a previously reported method.<sup>15</sup> Additional experimental details are provided in Supporting Information.

## Results and Discussion

To characterise the core-shell nanoparticles used, high resolution TEM images were obtained (Figure 2). An average core diameter of  $38.3 \pm 5.7$  nm was observed and the shells were  $9.7 \pm 2.5$  nm, while some asymmetric growth was occasionally observed. The distribution of elements was probed by EDX mapping in STEM-HAADF mode (Figure 2b

inset) showing that gold is clearly concentrated within the core of the nanoparticles and surrounded by a silver shell.

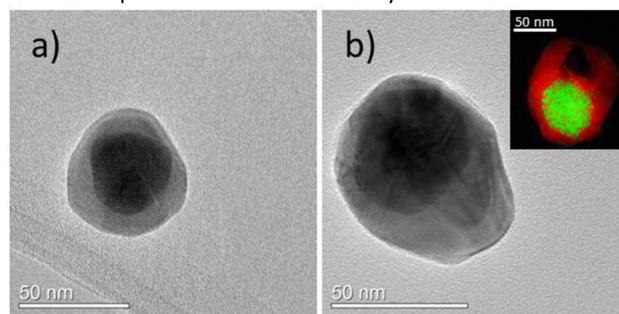


**Figure 2.** TEM bright field images of core-shell nanoparticles showing the gold cores (darker regions) encapsulated by silver shells (lighter regions). An EDX map obtained using STEM-HAADF mode is shown in the inset of (b) identifying the distribution of silver (red) and gold (green).

The electrochemical behaviour of the core-shell nanoparticles was tested in a range of solutions (Figure 3). The cyclic voltammogram recorded in 0.1 M NaCl solution (Figure 3a) shows a distinctive silver oxidation peak at 0.08 V (vs SCE).<sup>16,17</sup> At more positive potentials (ca. 1.0 V) a broad oxidation peak is present which is attributed to the oxidation of both bromide to bromine from the CTAB present in the nanoparticle solution<sup>18</sup> as well as the oxidation of gold to gold bromide species.<sup>19</sup> The reduction of bromine is then seen on the reverse scan at ca. 0.86 V, followed by a small reduction peak at ca. 0.53 V due to the reduction of gold oxidised in the forward scan. The charge associated with the oxidation of silver in the forward scan was found to be  $0.62 \mu C \mu L^{-1}$  drop cast (Table 1).

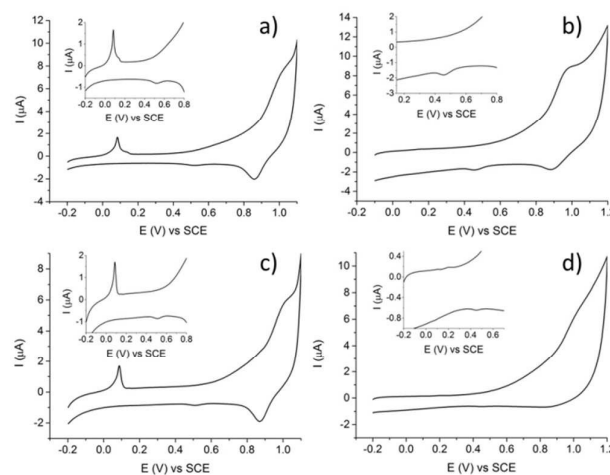
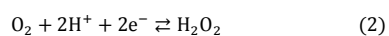


**Figure 3.** Cyclic voltammograms of gold-core silver-shell nanoparticles on glassy carbon substrates in 0.1 M NaCl (a), 0.1 M  $HNO_3$  (b), 0.1 M HCl (c) and 0.1 M  $NaNO_3$  (d), recorded at a scan rate of  $50 \text{ mV s}^{-1}$ .

The voltammetry of the core-shell nanoparticles was then tested in 0.1 M  $HNO_3$  (Figure 3b). From this it can be seen that no silver was detected electrochemically. This absence of a silver oxidation signal may have resulted from either the chemical dissolution of silver or the loss of nanoparticles from

the electrode surface during the experiment, which may have been partially facilitated by the dissolution of the silver shells. Importantly, however, a gold reduction peak is present,<sup>20</sup> which evidences that the absence of a silver oxidation peak is *not* due to the loss of nanoparticles from the electrode surface but rather that the silver shells were chemically dissolved.

The mechanism of silver dissolution under such conditions has been debated in the literature, as it has been postulated that the reduction of oxygen provides the electrons required for silver dissolution through either a two or four electron process. Recent work has suggested that due to the rapid mass transport which occurs at nanoparticle surfaces the reduction of O<sub>2</sub> is limited by the fast diffusion of H<sub>2</sub>O<sub>2</sub> from the nanoparticle surface,<sup>21,22</sup> so the dissolution of Ag (Equation 1) is driven here by the reaction in Equation 2.



The concentration of dissolved O<sub>2</sub> in 0.1 M HNO<sub>3</sub> was determined by voltammetry at a range of scan rates (Figure S1, Supporting Information) and analysis using the irreversible Randles-Ševčík equation,<sup>23</sup> from which it was found that a concentration of 7 μM was present even when the solution had been thoroughly purged with N<sub>2</sub> prior to performing the experiments. This value is three orders of magnitude greater than the concentration of O<sub>2</sub> required (10.4 nM) to oxidise the silver present on the electrode surface, and can therefore explain the complete dissolution of silver observed in 0.1 M HNO<sub>3</sub>.

**Table 1.** Normalised electrochemical silver oxidation and gold reduction charges for core-shell nanoparticles in different solutions. Values given are the mean values of at least 5 repeats ± the standard deviation of the mean.

Solution	Ag oxidation charge (μC μL <sup>-1</sup> )	Au reduction charge (nC μL <sup>-1</sup> )	Normalised Ag oxidation charge
0.1 M HCl	0.52±0.06	64.2±11.9	1.00±0.21
0.1 M NaCl	0.62±0.02	117.5±16.1	0.64±0.09
0.1 M HNO <sub>3</sub>	0	44.4±7.1	0
0.1 M NaNO <sub>3</sub>	0.03±0.01	11.6±2.5	0.28±0.12

The voltammetry of core-shell nanoparticles in a 0.1 M HCl solution is shown in Figure 3c, where a distinctive silver oxidation peak is evident. The concentration of O<sub>2</sub> was again measured (Figure S2) and found to be 35 μM, and as the concentrations of O<sub>2</sub> and H<sup>+</sup> were similar to the 0.1 M HNO<sub>3</sub> case the dissolution of silver may be expected in 0.1 M HCl. However the introduction of Cl<sup>-</sup> clearly inhibits this dissolution, with similar silver oxidation charges observed in 0.1 M HCl compared with 0.1 M NaCl (as confirmed by Student's t-test, where p=0.14). Thus it is hypothesised that the chemical oxidation of the silver surface results in the formation of an insoluble and protective silver chloride layer. This layer is then electrochemically reduced at the start of the cyclic voltammogram, allowing the quantitative oxidation of silver to be measured in the forward scan. It should be noted that while

the results presented here relate to CTAB-capped nanosilver, this method may be directly utilised to study the stability of silver nanoparticles with a wide range of capping agents.

Having seen the stabilising influence of Cl<sup>-</sup> under these conditions, the dissolution of silver was probed in 0.1 M NaNO<sub>3</sub> (Figure 3d) where no added H<sup>+</sup> or Cl<sup>-</sup> were present. Here a very small silver oxidation peak was observed (0.03 μC μL<sup>-1</sup>), however it is also clear from the small gold reduction peak in the reverse scan that some nanoparticles have been lost from the electrode surface. This highlights the advantages of the use of core-shell nanoparticles to study the dissolution of nano-silver, as the loss of nanoparticles can be accounted for by the gold reduction charge. The normalised silver oxidation values (based on the ratio of the silver oxidation and gold reduction charges) are shown in Table 1, allowing for direct and quantitative comparison of the data. It is apparent that while similar values were obtained in the presence of 0.1 M HCl and 0.1 M NaCl, the normalised silver oxidation value was much lower in the presence of 0.1 M NaNO<sub>3</sub>, which can be directly ascribed to the dissolution of silver in this system. As the concentration of H<sup>+</sup> in 0.1 M NaNO<sub>3</sub> (pH 6.3) is two orders of magnitude higher than required for the reduction of O<sub>2</sub> to H<sub>2</sub>O<sub>2</sub>, this confirms that trace quantities of O<sub>2</sub> and H<sup>+</sup> can lead to the dissolution of nano-silver. These results also clearly show the stabilising effect that Cl<sup>-</sup> can have on nano-silver, necessitating that caution must be used when studying the dissolution of silver even in low concentrations of Cl<sup>-</sup>.

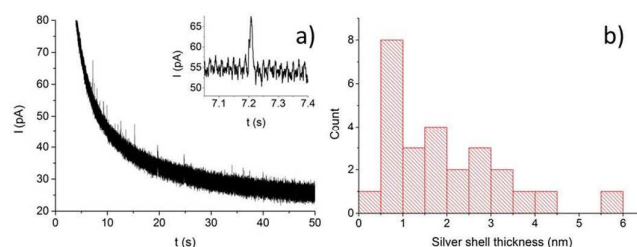


**Figure 4.** Chronoamperogram recorded in a solution of 90 fM gold-core silver-shell nanoparticles in 20 mM NaCl at 0.4 V vs a Ag quasi-reference electrode (a), with the calculated silver shell thickness in (b).

The electrochemical study of the core-shell nanoparticles was also extended using nano-impact experiments, where the Brownian motion driven collision of individual nanoparticles with an electrode surface allows their electrochemical behaviour to be analysed. Such experiments are extremely well suited to study the effect of nanoparticle aggregation on dissolution/passivation processes,<sup>7</sup> and are readily applicable to ultra-low (even femtomolar, as used here) nanoparticle concentrations.<sup>15,24</sup> Results of this study in 20 mM NaCl are shown in Figure 4, where a chronoamperogram displaying multiple nanoparticle impact events is seen in Figure 4a. The applied potential was chosen so that the charges associated with the impacts relate to the oxidation of silver on individual core-shell nanoparticles (Cyclic voltammogram shown in Figure S3). It should be noted that the normalised silver oxidation

charge determined in 20 mM NaCl ( $0.71 \pm 0.11$ ) was similar to the result shown previously for 0.1 M NaCl (as confirmed by Student's t-test, where  $p=0.66$ ), demonstrating that the dissolution of silver was again inhibited under these conditions. The thicknesses of the silver shells were then calculated from the nanoimpact experiments (Figure 4b), and the measured thicknesses ( $1.9 \pm 1.3$  nm) were found to be smaller than the expected value ( $9.7 \pm 2.5$  nm). This can be attributed to the larger diffusion coefficient of the smaller nanoparticles of the non-monodisperse 'solution-phase' ensemble as well as the  $O_2$  reduction driven formation of a AgCl protective shell, resulting in a lower electrochemical oxidation charge for the impacting individual nanoparticles.

## Conclusions

The oxidative dissolution of silver was shown to be driven by the reduction of oxygen, even in the presence of micromolar concentrations of oxygen still present after extensive bubbling with nitrogen. This dissolution is inhibited in the presence of low concentrations of chloride, through the formation of a protective AgCl layer on the nanoparticle surface. Studies were also extended to the single nanoparticle level where the thickness of individual silver shells was determined, showing the depth of information which can be provided through electrochemical approaches. These findings evidence the critical role that the solution chemistry plays towards the stability of nano-silver, with the method presented providing a convenient route to overcome existing controversies in the literature. In addition this work highlights the exceptional strengths of electrochemical methods to study the fate of nano-silver in various media, and may be readily adapted to investigate the behaviour of other nanosized materials. As such this approach provides great scope to rigorously probe the fate of a wide variety of state-of-the-art multifunctional core-shell nanomaterials across a broad range of experimental conditions.

## Acknowledgements

The support of this work through a Marie Curie International Incoming Fellowship (BJP, Project number 630069) and a Marie Curie Intra European Fellowship (KT, Project number 327706) are gratefully acknowledged.

## Notes and References

- 1 J. Fabrega, S. N. Luoma, C. R. Tyler, T. S. Galloway and J. R. Lead, *Environ. Int.*, 2011, **37**, 517-531.
- 2 K. A. Huynh and K. L. Chen, *Environ. Sci. Technol.*, 2011, **45**, 5564-5571.
- 3 X. Li, J. J. Lenhart and H. W. Walker, *Langmuir*, 2011, **28**, 1095-1104.
- 4 J. Liu and R. H. Hurt, *Environ. Sci. Technol.*, 2010, **44**, 2169-2175.
- 5 Z.-M. Xiu, Q.-B. Zhang, H. L. Puppala, V. L. Colvin and P. J. Alvarez, *Nano Lett.*, 2012, **12**, 4271-4275.

- 6 J. Liu, D. A. Sonshine, S. Shervani and R. H. Hurt, *ACS Nano*, 2010, **4**, 6903-6913.
- 7 W. Zhang, Y. Yao, N. Sullivan and Y. Chen, *Environ. Sci. Technol.*, 2011, **45**, 4422-4428.
- 8 Z.-M. Xiu, J. Ma and P. J. Alvarez, *Environ. Sci. Technol.*, 2011, **45**, 9003-9008.
- 9 X. Li, J. J. Lenhart and H. W. Walker, *Langmuir*, 2010, **26**, 16690-16698.
- 10 C. Levard, S. Mitra, T. Yang, A. D. Jew, A. R. Badireddy, G. V. Lowry and G. E. Brown Jr, *Environ. Sci. Technol.*, 2013, **47**, 5738-5745.
- 11 K. Loza, J. Diendorf, C. Sengstock, L. Ruiz-Gonzalez, J. M. Gonzalez-Calbet, M. Vallet-Regi, M. Koller and M. Epple, *J. Mater. Chem. B*, 2014, **2**, 1634-1643.
- 12 A. D. Dwivedi, S. P. Dubey, M. Sillanpää, Y.-N. Kwon, C. Lee and R. S. Varma, *Coord. Chem. Rev.*, 2015, **287**, 64-78.
- 13 K. Tschulik, C. Batchelor-McAuley, H.-S. Toh, E. J. Stuart and R. G. Compton, *Phys. Chem. Chem. Phys.*, 2014, **16**, 616-623.
- 14 W. Z. Teo and M. Pumera, *RSC Adv.*, 2014, **4**, 5006-5011.
- 15 J. Ellison, C. Batchelor-McAuley, K. Tschulik and R. G. Compton, *Sensor. Actuat. B-Chem.*, 2014, **200**, 47-52.
- 16 M. Gulppi, J. Pavez, J. H. Zagal, M. Sancy, M. Azocar, F. Scholz and M. A. Páez, *J. Electroanal. Chem.*, 2015, **745**, 61-65.
- 17 N. K. Chaki, J. Sharma, A. Mandle, I. Mulla, R. Pasricha and K. Vijayamohanan, *Phys. Chem. Chem. Phys.*, 2004, **6**, 1304-1309.
- 18 S. Corona-Avenidaño, M. T. Ramírez-Silva, M. Palomar-Pardavé, L. Hernández-Martínez, M. Romero-Romo and G. Alarcón-Ángeles, *J. Appl. Electrochem.*, 2010, **40**, 463-474.
- 19 D. Han, S.-S. Kim, Y.-R. Kim, B.-H. Sohn and T. D. Chung, *Electrochem. Commun.*, 2015, **53**, 11-14.
- 20 Note that the gold reduction peak is analysed in preference to the gold oxidation peak as the oxidation of bromide complicates the analysis of the latter feature.
- 21 C. C. M. Neumann, E. Laborda, K. Tschulik, K. R. Ward and R. G. Compton, *Nano Res.*, 2013, **6**, 511-524.
- 22 C. Batchelor-McAuley, K. Tschulik, C. C. Neumann, E. Laborda and R. G. Compton, *Int. J. Electrochem. Sci.*, 2014, **9**, 1132-1138.
- 23 R. Nissim and R. G. Compton, *ChemElectroChem*, 2014, **1**, 763-771.
- 24 J. C. Lees, J. Ellison, C. Batchelor-McAuley, K. Tschulik, C. Damm, D. Omanović and R. G. Compton, *ChemPhysChem*, 2013, **14**, 3895-3897.